NLR TP 96748

Airfoil design and optimization methods: recent progress at NLR

B.I. Soemarwoto and Th.E. Labrujère

DOCUMENT CONTROL SHEET

	ORIGINATOR'S REF. NLR TP 96748 U		SECURITY CLASS. Unclassified

ORIGINATOR
National Aerospace Laboratory NLR, Amsterdam, The Netherlands

TITLE
Airfoil design and optimization methods: recent progress at NLR

AUTHORS B.I. Soemarwoto and Th.E. Labrujère	DATE 970129	pp ref 21 15

DESCRIPTORS

Airfoils	Navier-Stokes equation
Constraints	Optimization
Design analysis	Pressure drag
Drag reduction	Quadratic programming
Euler equations of motion	Transonic flow
Lagrange multipliers	Turbulence model
	Two dimensional bodies

ABSTRACT
The present paper considers the problem of aerodynamic airfoil shape
optimization where the shape of an airfoil is to be determined such that
a priori specified design criteria are formulated by defining an
objective or cost function, the minimum of which represents the solution
to the design problem.
A survey is given of developments at NLR applying the adjoint operator
approach, utilizing a compressible inviscid flow model based on the Euler
equations and a compressible viscous flow model based on the Reynolds-
Averaged Navier-Stokes equations. Computational results are presented for
a two-point drag-reduction design problem.

Contents

5 Figures

(21 pages in total)

Summary

The present paper considers the problem of aerodynamic airfoil shape optimization where the shape of an airfoil is to be determined such that a priori specified design criteria will be met to the best possible extent. The design criteria are formulated by defining an objective or cost function, the minimum of which represents the solution to the design problem.

A survey is given of developments at NLR applying the adjoint operator approach, utilizing a compressible inviscid flow model based on the Euler equations and a compressible viscous flow model based on the Reynolds-Averaged Navier-Stokes equations. Computational results are presented for a two-point drag-reduction design problem.

This page is intentionally left blank.

1 Introduction

At NLR, successful computational methods for the design of airfoils and wings in subsonic and transonic flow have been developed following the residual-correction approach (Ref. 4). Essentially, these methods are based on solving an inverse problem, determining an airfoil or wing shape such that it will generate a priori prescribed surface pressure distributions at given operating conditions. The design goals, expressed in terms of these prescribed target pressure distributions, are approximated to the best possible extent, taking into account additional requirements with respect to the geometry. During the iteration process of solving the design problem, for each new estimate of the airfoil or wing geometry, the surface pressure distribution is analyzed at each desired operating condition and from the differences with the target pressure distributions a new estimate of the geometry is determined. This way of specifying the design goals gives the designer direct control over local flow properties, but constraints with respect to global characteristics as drag- or lift-coefficients are specified less easily. The main advantage of the NLR residual-correction methods is the fact that in each iteration step leading to a new estimate of the geometry only one flow computation is required.

A more straightforward, direct approach to solve the airfoil or wing design problem is obtained by posing the design problem as the minimization (or maximization) problem of an objective functional subject to a number of design constraints. The advantage of this approach is that it offers a great deal of flexibility with respect to the form in which the design goals should be expressed; it is not restricted to design goals in terms of target pressure distributions. Moreover, in principle any combination and number of appropriate design objectives may be specified.

Usually, minimization problems are solved most efficiently by making use of the gradient of the objective functional with respect to the design variables. If this gradient is determinied by numerical differentiation, such as pioneered by Hicks et.al. 6, the application of this type of minimization is limited to problems involving only a small number of design variables, simply because of otherwise prohibitively high computing costs. Gradient-based minimization involving larger numbers of design variables is feasible only, when the gradient is determined analytically as e.g. in Drela's method for the design of airfoils in Euler flow, which is based on Newton-iteration 3.

The most efficient approach to solve design problems formulated as optimization problems, seems to be the approach based on optimal control theory, which is also commonly referred to as the variational method, as described by Jameson for airfoil and wing design 9. Following this type of approach (see e.g. Refs. 12, 10, 8, 7), a design method based on the Euler and Reynolds-averaged

Navier-Stokes (RANS) equations has been developed at NLR (Ref. 14). The feasibility of the method is investigated for transonic single- and multi-point design problems.

The design problem is solved by means of an iteration process, involving at each iteration step the solution of a flow problem for the state variables, the solution of an adjoint problem for the adjoint variables and the determination of a new estimate of the geometry. In terms of computational costs this approach comes in line with the residual-correction approach because of the fact that for a geometry update in principle only one flow problem and one adjoint problem (of about the same computational effort as the flow problem) have to be solved.

The design methodology presented in this paper takes advantage of the availability of a flow solver and an optimization routine that requires the function value and gradient. The gradient of the aerodynamic functionals are computed by means of the variational method. The formulation of the adjoint problem, the construction of an adjoint solver for obtaining the Lagrange multipliers and the gradient, and the integration of the adjoint solver with the existing flow solver and optimization routine form the main subject of the investigation.

This paper describes experiences obtained with applications of the present design method to aerodynamic airfoil design problems utilizing a compressible inviscid flow model based on the Euler equations and a compressible viscous flow model based on the RANS equations. The capability of the approach to address multi-point design problems is demonstrated by considering a two-point airfoil drag reduction problem for transonic flow.

2 Formulation of the Gradient by means of the Variational Method

The design problems are posed as optimization problems involving aerodynamic functionals representing the lift (C_l), drag (C_d), and pitching moment (C_m) coefficients. These are defined in terms of the pressure coefficient C_p obtained from the flow variables $\mathbf{Q}$ which satisfy the flow equations.

The design variables consist of geometric parameters $\boldsymbol{\theta}$ (defining the airfoil geometry) and an angle of attack α (defining the orientation of the free stream with respect to the airfoil geometry). The optimal values of $\boldsymbol{\theta}$ and α are obtained by means of a gradient-based optimization algorithm. The gradients of the aerodynamic functionals with respect to the design variables $\boldsymbol{\theta}$ and α are computed by means of the variational method.

The optimization problem being addressed can be written as follows[1],

$$\text{Minimize} \quad \mathcal{P}(\mathbf{Q}, \boldsymbol{\theta}, \alpha), \tag{1}$$

Subject to:

$$\begin{aligned} \mathcal{A}(\mathbf{Q}, \boldsymbol{\theta}, \alpha) &\leq 0, \\ \mathbf{G}(\boldsymbol{\theta}) &\leq 0, \end{aligned}$$

where $\mathcal{P}$ and $\mathcal{A}$ represent such aerodynamic functionals as lift, drag and pitching moment coefficients, while the vector $\mathbf{G}$ represents geometric constraints. The geometric parameters $\boldsymbol{\theta}$ and the angle of attack α are treated as the design variables, of which the optimal values are to be determined.

Problem (1) is subject to the flow equations for a given (fixed) value of the Mach number and Reynolds number, which impose an implicit dependency of the flow variables $\mathbf{Q}$ upon $\boldsymbol{\theta}$ and α.

Problem (1) is to be solved by means of a gradient-based optimization algorithm. The gradient of $\mathbf{G}$ can be obtained rather easily by direct analytical differentiation, whereas the gradients of the aerodynamic functionals $\mathcal{P}$ and $\mathcal{A}$ are computed by means of the variational method. This implies that an adjoint problem must be formulated, the solution of which is used for evaluating the gradients. Figure (1) illustrates the nomenclature. The time-dependent flow equations can be

---

[1] †For the sake of brevity, the Mach number and Reynolds number (in the case of viscous flow) do not appear because these are assumed fixed.

written in the form:

$$\frac{\partial \mathbf{Q}}{\partial t} + \vec{\nabla} \cdot \vec{\mathbf{F}} = 0, \quad \text{in } \Omega, \tag{2}$$

where $\mathbf{Q}$ is the vector of conservative flow variables:

$$\mathbf{Q} = \begin{pmatrix} \rho \\ \rho u \\ \rho v \\ \rho E \end{pmatrix}. \tag{3}$$

At the steady-state, equation (2) becomes

$$\vec{\nabla} \cdot \vec{\mathbf{F}} = 0. \tag{4}$$

The vector $\vec{\mathbf{F}}$ represents the mass, momentum, and energy fluxes. The flow equations are subject to the boundary conditions on the airfoil surface S_a, which can be expressed as a vector equation:

$$\mathbf{B} = 0. \tag{5}$$

For *an inviscid flow*, equation (2) represents the Euler equations, while equation (5) represents the zero normal-velocity boundary condition such that $\mathbf{B}$ is a one-dimensional vector. For *a viscous flow*, equation (2) represents the Reynolds-Averaged Navier-Stokes equations, while equation (5) represents the no-slip and the adiabatic wall boundary conditions. In this case, $\mathbf{B}$ is a vector with three elements.

For the design cases to be considered, a general form of aerodynamic functionals is assumed as follows

$$\mathcal{F} = \int_{S_a} \psi(p, \boldsymbol{\theta}, \alpha) \, dS. \tag{6}$$

where ψ is a function of the pressure p, the design variables $\boldsymbol{\theta}$, and the angle of attack α. The

notation $\mathcal{F}$ applies to both $\mathcal{P}$ and $\mathcal{A}$ of the problem statement (1).

Employing the variational method means that the adjoint equation must be formulated, the solution of which provides the Lagrange multipliers. These in turn are used in evaluating the gradient of the functional with respect to the design variables θ and α.

As p is obtained from $\mathbf{Q}$ which satisfies the steady-state flow equations, the functional $\mathcal{F}$ is independent of the transient state. Therefore, it is sufficient to consider the steady-state flow equations (4) and boundary condition (5) in the definition of a Lagrangian $\mathcal{L}$ as follows,

$$\mathcal{L} = \int_{S_a} \psi \, dS + \int_{\Omega} \boldsymbol{\lambda} \cdot (\vec{\nabla} \cdot \vec{\mathbf{F}}) \, d\Omega + \int_{S_a} \boldsymbol{\Upsilon} \cdot \mathbf{B} \, dS, \tag{7}$$

where $\boldsymbol{\lambda}$ and $\boldsymbol{\Upsilon}$ are the Lagrange multipliers. $\boldsymbol{\lambda}$ is a vector with four components defined in Ω, each component of which may be considered as corresponding to a component of the conservative flow variables $\mathbf{Q}$. The Lagrange multiplier $\boldsymbol{\Upsilon}$ is defined on S_a. In the case of inviscid flow, $\boldsymbol{\Upsilon}$ consists of one element, whereas for viscous flow $\boldsymbol{\Upsilon}$ consists of three elements.

In order to derive the adjoint and gradient equations, one must evaluate the variation of $\mathcal{L}$, denoted as $\delta\mathcal{L}$, due to the independent variables $\boldsymbol{\lambda}$, $\boldsymbol{\Upsilon}$, $\mathbf{Q}$, θ and α:

$$\delta\mathcal{L} = \delta\mathcal{L}_{\lambda} + \delta\mathcal{L}_{\Upsilon} + \delta\mathcal{L}_{Q} + \delta\mathcal{L}_{\theta} + \delta\mathcal{L}_{\alpha}.$$

The notation $\delta\mathcal{L}_{\lambda}$ refers to the variation of $\delta\mathcal{L}$ implied by the variation of λ while the other variables are kept fixed, and similarly for $\delta\mathcal{L}_{\Upsilon}$, etc. The contribution of the variation of $\boldsymbol{\lambda}$ and $\boldsymbol{\Upsilon}$ are eliminated as the flow equation (4) and the boundary condition (5) are satisfied. The adjoint equation and boundary conditions are obtained by setting $\delta\mathcal{L}_{Q}$ equal to zero, which also leads to the relations between $\boldsymbol{\Upsilon}$ and $\boldsymbol{\lambda}$.

After solving the flow and the adjoint equations, providing the values of $\mathbf{Q}$, $\boldsymbol{\lambda}$ and $\boldsymbol{\Upsilon}$, the variation of $\mathcal{L}$ becomes

$$\delta\mathcal{L} = \delta\mathcal{L}_{\theta} + \delta\mathcal{L}_{\alpha}. \tag{8}$$

By direct analytical differentiation, the gradient of $\mathcal{F}$ with respect to θ and to α can be obtained.

These are expressed as, respectively,

$$\frac{d\mathcal{F}}{d\boldsymbol{\theta}} = \lim_{\delta\boldsymbol{\theta}\to 0} \frac{\delta\mathcal{L}_\theta}{\delta\boldsymbol{\theta}} = \frac{\partial\mathcal{L}}{\partial\boldsymbol{\theta}},$$ (9)

and

$$\frac{d\mathcal{F}}{d\alpha} = \lim_{\delta\boldsymbol{\theta}\to 0} \frac{\delta\mathcal{L}_\alpha}{\delta\alpha} = \frac{\partial\mathcal{L}}{\partial\alpha}.$$ (10)

For the case with a fixed (design) lift coefficient, the following condition holds

$$\left(\frac{dC_l}{d\alpha}\right)\delta\alpha + \left(\frac{dC_l}{d\boldsymbol{\theta}}\right)\cdot\delta\boldsymbol{\theta} = 0.$$

This implies that one variable out of the set of the components of $\boldsymbol{\theta}$ and α can be chosen to be dependent. A convenient choice is to take α as the dependent variable, giving

$$\delta\alpha = -\left(\frac{dC_l}{d\alpha}\right)^{-1}\left(\frac{dC_l}{d\boldsymbol{\theta}}\right)\cdot\delta\boldsymbol{\theta}.$$ (11)

The variation of the Lagrangian is now expressed as

$$\delta\mathcal{L} = \delta\mathcal{L}_\theta + \delta\mathcal{L}_\alpha = \left(\frac{d\mathcal{F}}{d\boldsymbol{\theta}}\right)\cdot\delta\boldsymbol{\theta} + \left(\frac{d\mathcal{F}}{d\alpha}\right)\delta\alpha.$$ (12)

Substitution of equation (11) gives

$$\delta\mathcal{L} = \left(\frac{d\mathcal{F}}{d\boldsymbol{\theta}}\right)\cdot\delta\boldsymbol{\theta} - \left(\frac{d\mathcal{F}}{d\alpha}\right)\left(\frac{dC_l}{d\alpha}\right)^{-1}\left(\frac{dC_l}{d\boldsymbol{\theta}}\right)\cdot\delta\boldsymbol{\theta}.$$

Hence, for a fixed C_l the gradient of $\mathcal{F}$ with respect to the design variables $\boldsymbol{\theta}$ can be obtained as

$$\left(\frac{d\mathcal{F}}{d\boldsymbol{\theta}}\right)_{C_l} = \frac{d\mathcal{F}}{d\boldsymbol{\theta}} - \left(\frac{d\mathcal{F}}{d\alpha}\right)\left(\frac{dC_l}{d\alpha}\right)^{-1}\left(\frac{dC_l}{d\boldsymbol{\theta}}\right),$$ (13)

with $\left(\frac{d\mathcal{F}}{d\boldsymbol{\theta}}\right)$ given by equation (9), and $\left(\frac{d\mathcal{F}}{d\alpha}\right)$ by equation (10). The expressions for $\left(\frac{dC_l}{d\alpha}\right)$ and $\left(\frac{dC_l}{d\boldsymbol{\theta}}\right)$ are obtained by taking C_l for $\mathcal{F}$.

NLR

3   Computer Implementation

The present investigation makes use of the HI-TASK code of the National Aerospace Laboratory NLR (Refs. 1 and 5). HI-TASK, which stands for **H**ighly-**I**ntegrated **T**urbulent **A**irflow **S**imulation **K**ernel, is basically a 2-D flow solver for single-element airfoil applications based on the Reynolds-averaged Navier-Stokes (RANS) equations, employing the Baldwin-Lomax turbulence model. The Euler mode of the code is obtained by dropping the viscous fluxes.

The discretization in HI-TASK is based on a cell-vertex finite volume scheme equivalent with a central difference scheme. The steady-state flow solution is obtained by integrating the time-dependent flow equations using the five-stage Runge-Kutta scheme with a V-cycle multigrid procedure. For the stability of the central-difference scheme, 4-th order dissipation terms are introduced, while 2-nd order dissipation terms are added for capturing shock waves. The dissipation terms are formulated based on the work of Jameson et al. 11.

The discretization of the adjoint equations and the computer implementation are chosen such that maximum advantage is taken of the existing features of HI-TASK. The philosophy is to treat the flow solver as a black box. This leads to a similar discretization scheme for solving the adjoint equation as that for solving the flow equations. Also, the dissipation terms can be formulated in the same way as that for the flow equations.

The present investigation employs the optimization routine FSQP, which stands for **F**easible **S**equential **Q**uadratic **P**rogramming. This routine is based on a modified Sequential Quadratic Programming (SQP) algorithm capable of generating feasible iterates. The routine requires as input the objective and constraint function values and the gradients. The detailed description of the algorithm used in FSQP is given in Ref. (15). Apart from the consideration that SQP is generally known to be the most cost-effective method for non-linear constrained optimization, the reasons for selecting FSQP are the followings,

(i) FSQP generates feasible iterates with respect to constraints. This has a practical advantage that,—if the optimization process should be stopped at an intermediate stage—, the last iterate would still be useful in the sense that it would represent an improvement over the initial design while the constraints are satisfied.

(ii) If the initial design provided by the designer is infeasible for some inequality constraints, FSQP first generates a feasible iterate before minimizing the objective. This offers convenience if the designer is primarily concerned about the constraints.

(iii) FSQP has the capability of solving multi-objective optimization problems in a $min\text{-}max$

sense. This is suitable for dealing with multi-point aerodynamic design to be described in Section 4.

In order to solve an airfoil design problem, the airfoil geometry must be parameterized. A parameterization scheme should satisfy the following requirements:

(i) In principle there should be no restriction on the possible number of design variables. This is desirable in order not to restrict the design space to a certain family of airfoil shapes.

(ii) The surface curvature must be continuous to ensure smoothness of the airfoil surface. This is desirable so as to avoid numerical irregularities that could be implied by surface discontinuities.

(iii) The design variables should preferably have (in an approximate sense) a linear relationship with the surface curvature. This is expected to have an effect of reducing the non-linearity of the optimization problem, considering that, for local subsonic flow, a local variation of the surface curvature is proportional (in an approximate sense) with the local variation of pressure (Refs.2, 13), while the aerodynamic functionals of interest are defined in terms of pressure. This consideration can be expected also to be relevant for transonic conditions because the flow is locally subsonic over a large part of the airfoil surface.

In the present investigation, these requirements have led to a shape parameterization scheme which generates an airfoil geometry with C_2 surface continuity (Ref. 14).

4 Computational Results

In order to demonstrate the suitability of the present design method for multi-point airfoil design problems, Case ME and MN are defined for an inviscid and a viscous flow, respectively. The design points are specified as follows:

- Design Point 1 (DP-1): $C_l = 1.$, $M_\infty = 0.72$, Re $= 6.5 \times 10^6$.
- Design point 2 (DP-2): $C_l = 0.5$, $M_\infty = 0.78$. Re $= 6.5 \times 10^6$.

The Reynolds number, Re, is not applicable in the Euler case. The objective is to reduce the pressure drag (C_{d_1} and C_{d_2}) while satisfying constraints on the pitching moments (C_{m_1} and C_{m_2}) in both design points. Geometric constraints are imposed, limiting the value of the leading-edge radius, the trailing-edge angle, and the cross-sectional area of the airfoil. The optimization starts with an initial airfoil specified as a best-fit of the RAE 2822 airfoil. The optimization begins with all constraints active.

In order to be representative for a real multi-disciplinary design practice, in which compromise might have to be accepted, it is assumed that, in reducing the drag, a certain amount of violation of the pitching moment constraint (i.e. the aerodynamic constraint) is allowed in favour of strictly satisfying the geometric constraint (e.g. due to structural requirements). Then, the multi-point design problem can be posed as a *fuzzy* optimization problem. Here, the so-called membership function μ, $0 \leq \mu \leq 1$, is introduced for representing the aerodynamic objective and constraint.

The form of membership function for the drag to be minimized is depicted in Figure 2(a), while that for the pitching moment constraint is shown in Figure 2(b). These apply to both design points, which can be interpreted as that a 75% reduction of drag is desirable while allowing a 10% violation of the pitching moment constraints.

In a fuzzy optimization involving a single membership function, one attempts to achieve the highest possible value of the membership function. If there are n membership functions, one attempts to achieve the highest possible value of the *minimum amongst the membership functions*, i.e.

$$\text{Maximize } \min(\mu_1, ..., \mu_n).$$

This can be interpreted as that, at any intermediate stage of optimization process, the criterion with the worst quality (i.e. with the smallest membership function) will be improved (i.e. maximized) ignoring (temporarily) the other criteria.

For the design case being considered, the fuzzy optimization problem can be expressed as a min-max problem as follows,

$$\text{Minimize} \quad max(-\mu(C_{d_1}), -\mu(C_{d_2}), -\mu(C_{m_1}), -\mu(C_{m_2})) \tag{14}$$

$$\text{subject to:} \quad \mathbf{G} \leq 0.$$

where $\mathbf{G}$ is the vector of geometric constraints. It is noted that the equivalent $min - max$ form has been chosen in order to maintain the compatibility with the optimization routine FSQP which is a minimizer.

4.1 Multi-point design based on the Euler equations

The drag and pitching moment coefficients are shown in Figure 3. An empty circle, referred to as "Evaluated", represents one geometry and one flow analysis. A cross, referred to as "New iterate", indicates that the corresponding geometry and flow analysis are used by the optimization algorithm as a basis for finding the next iterate. The gradient needs to be computed only for the crossed circles. The process from one crossed circle to another represents a so-called line search. As can be seen in the C_p distributions, the shock waves are indeed weaker in the final iterate. The optimization process was stopped after a maximum number of 20 flow analyses in a design point was exceeded. The obtained airfoil geometry is shown in Figure 4(a).

Figure 4(b) shows the history of the membership functions. In fuzzy optimization, the minimum amongst the membership function values corresponds to the most important criterion. The figure indicates that the membership function value of the pitching moment constraints is not the minimum for most iterates. Hence, for most iterates, the pitching moment constraints are not considered as important. This can be interpreted as that the 10% "leeway" provides ample room for the reduction of drag. The figure also indicates that, in the early stages of optimization, the drag in DP-2 was considered more important than in the other design point. This role is switched at the fifth iteration, where the first design point became more important. It is also indicated that taking one criterion (objective or constraint) as the most important one, does not necessarily mean that the other criteria must be compromised (e.g., from the 3rd to the 4th iteration all criteria are improved). As a matter of fact, the change in membership function from one iteration to another gives an indication of the "sensitivity" of the associated criterion with respect to the most important one.

In the final result a balanced reduction of drag is obtained, i.e. about 25% and 28% reduction in the first and the second design point, respectively. This is accompanied by about 3% and 5% violation

of the pitching moment constraints in the respective design points. The balanced reduction of drag is an expected result, because the drag values in the two design points are initially considered as equally bad, while it is desired to obtain an equal amount of improvement (75% reduction of drag).

4.2 Multi-point design based on the RANS equations

The drag and pitching moment coefficients are shown in Figure 5. Like in the Euler case, a balanced reduction of drag values has again been obtained, but with a smaller amount than for the inviscid case. About 12% and 10% drag reduction in the first and the second design point is achieved, respectively. This is accompanied by about 7% and 7.5% violation of the pitching moment constraints in the respective design points. In agreement with the drag reduction, the shock waves appear to be slightly weaker in the final C_p distributions.

5   Conclusions

The results given above indicate that the present method represents a viable approach for solving constrained transonic aerodynamic design (pressure drag reduction) problems, based on the compressible inviscid and viscous flow models described by the Euler and the RANS equations, respectively. The possibility for incorporating both aerodynamic and geometric constraints is of great practical value, since in real design practice one is always confronted with such design constraints.

The computational results indicate that (both aerodynamic and geometric) constraints tend to be more stringent in case of the viscous (RANS) flow model. This is to be expected, since in the Euler case there are no restrictions on the local pressure gradient while in the RANS case these are limited by the ability of the boundary-layer to cope with them without (significant) separation.

The complexity of multi-point design problems is not only incurred by conflicting aerodynamic objectives, but also by restrictions imposed by aerodynamic constraints. The fuzzy optimization method appears to be effective in alleviating the level of problem complexity, because the objectives and constraints are treated in the same way as the set of criteria which have to be achieved. This is measured in terms of membership functions. The results demonstrate that allowing relatively small constraint violations can lead to significant improvements in the objectives.

In the test cases considered in the present investigation, the design space was defined by 11 design variables. The sensitivity of the solutions to the number of design variables has not been investigated.

The present methodology is not limited to two-dimensional single airfoil problems, but can be extended in order to deal with multi-component airfoils and three-dimensional design problems. This would imply a drastic increase in the number of design variables. Then, there might be a need for an optimization routine dedicated to large-scale optimization problems.

6 References

1. F.J. Brandsma. Description of the method used by NLR. In Haase W. *et.al*, editor, *EUROVAL–A European Initiative on Validation of CFD Codes*, volume 42 of *Notes on Numerical Fluid Mechanics*. Vieweg, Brunswick, 1993.

2. W.H. Davis Jr. Technique for developing design tools from the analysis methods of computational aerodynamics. *AIAA Paper 79-1529*, July 1979.

3. M. Drela. *Two-Dimensional Transonic Aerodynamic Design and Analysis Using the Euler Equations*. PhD thesis, Massachusetts Institute of Technology, 1985.

4. J.M.J. Fray, J.W. Slooff, J.W. Boerstoel, and A. Kassies. Inverse method with geometric constraints for transonic aerofoil design. *Intl. J. Numerical Method in Engineering*, 22:327–339, 1986.

5. R. Hagmeijer. Grid adaption based on modified anisotropic diffusion equations formulated in the parametric domain. *J. of Computational Physics*, 115(1):169–183, Nov 1994.

6. R.M. Hicks, E.M. Murman, and G.N. Vanderplaats. *An Assessment of Airfoil Design by Numerical Optimization*. NASA TM X-3092, 1974.

7. J. Huan and V. Modi. Optimum design of minimum drag bodies in incompressible laminar. *Inverse Problems in Engineering*, 1:1–25, 1994.

8. A. Iollo and M.D. Salas. *Contribution to The Optimal Shape Design of Two-Dimensional Internal Flows wth Embedded Shocks*. ICASE Rep. no. 95-20, 1995.

9. A. Jameson. *Aerodynamic Design via control theory*. ICASE Rep. no. 88-64, 1988.

10. A. Jameson. Optimum aerodynamic design using control theory. *CFD Review*, pages 495–528, 1995.

11. A. Jameson, W. Schmidt, and E. Turkel. Numerical solutions of the euler equations by finite volume methods using runge-kutta time-stepping schemes. *AIAA Paper 81-1259*, 1981.

12. J. Reuther and A. Jameson. Aerodynamic shape optimization of wing and wing-body configurations using control theory. *AIAA Paper 95-0123*, January 1995.

13. L.A. Smith and R.L. Campbell. *A Method for The Design for Transonic Flexible Wings*. NASA TP 3045, 1990.

14. B.I. Soemarwoto. *Multi-Point Aerodynamic Design by Optimization*. PhD thesis, Delft University of Technology, 1996.

15. J.L. Zhou and A.L. Tits. *User's Guide for FSQP Version 3.3b: A FORTRAN Code for Solving Constrained Nonlinear (Minimax) Optimization Problems, Generating Iterates Satisfying All Inequality and Linear Constraints*. Electrical Engineering Department and Institute for Systems Research, University of Maryland.
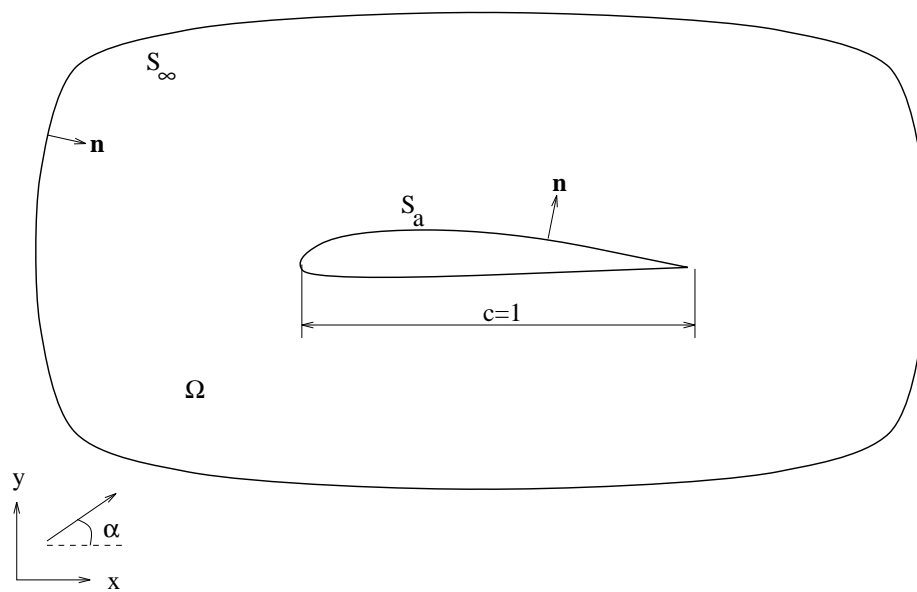
S_∞

n

n

S_a

c=1

Ω

y

α

x

Fig. 1   Domain definition of the flow field.

μ

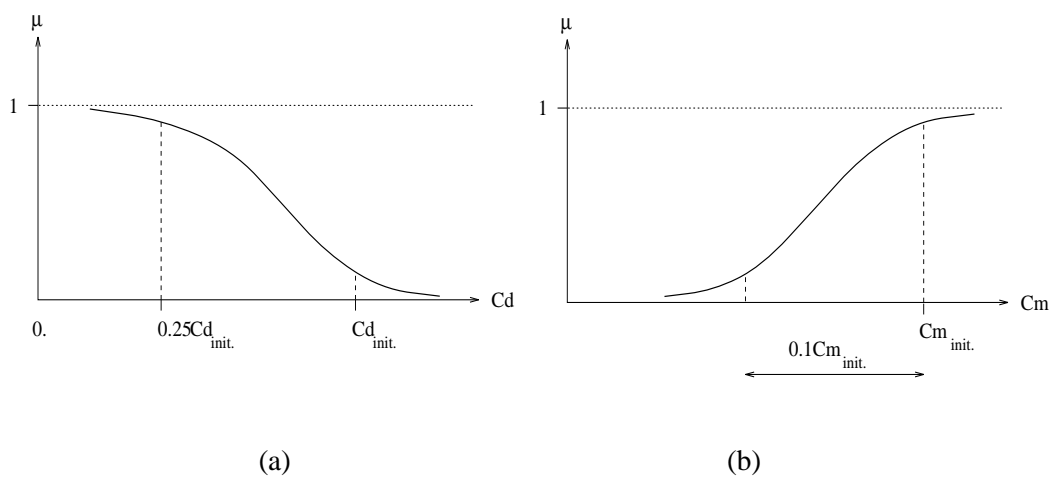1

0.

0.25Cd$_{init.}$

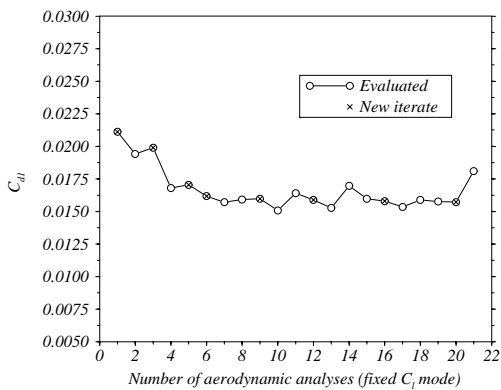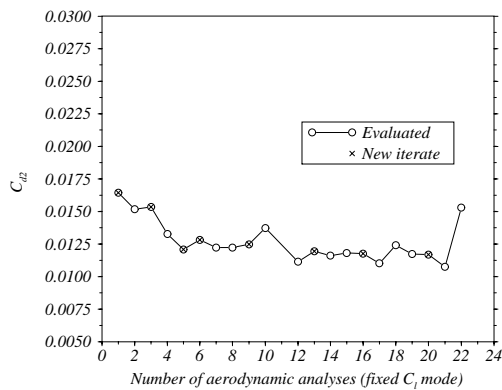Cd$_{init.}$
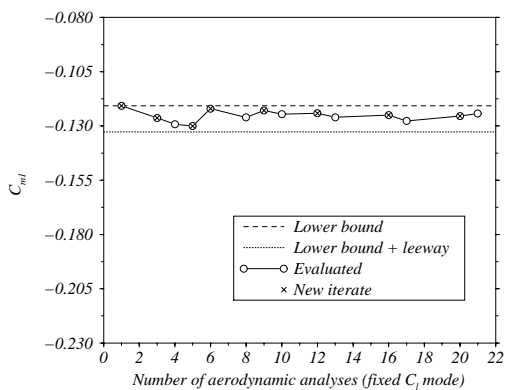
Cd

μ

1

0.1Cm$_{init.}$

Cm$_{init.}$

Cm

(a)
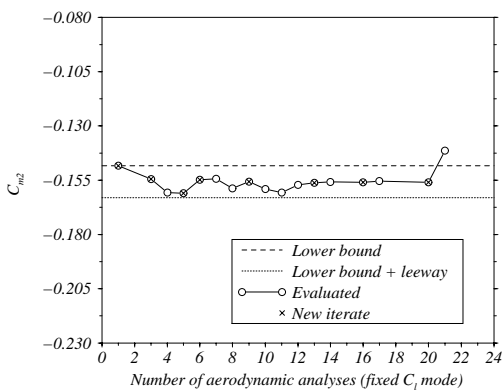
(b)

Fig. 2   Membership functions.
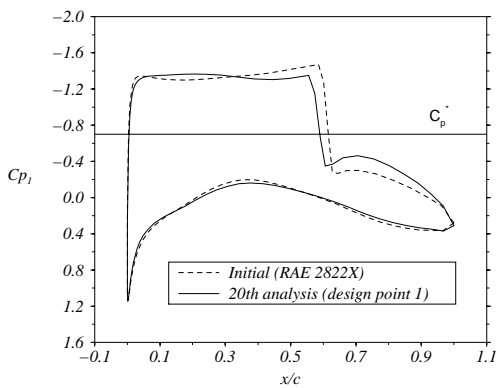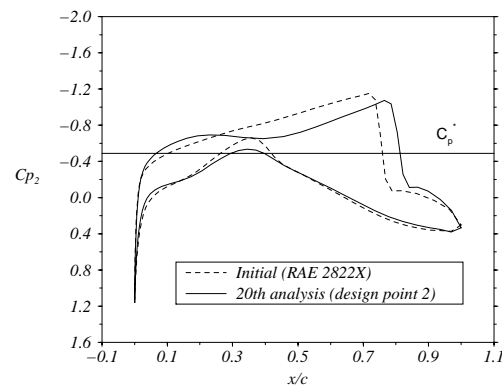
(a) C_d at DP-1

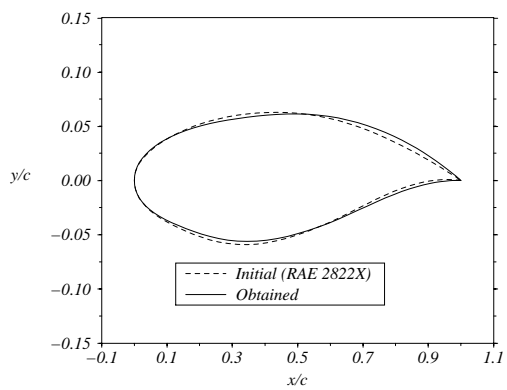(b) C_d at DP-2

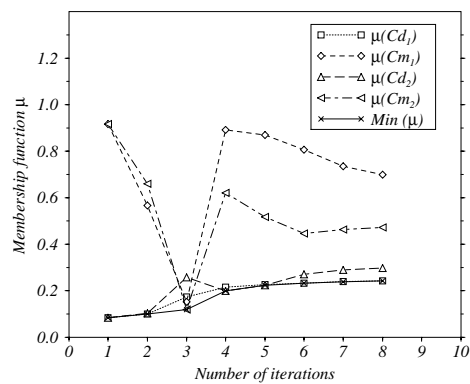(c) C_m at DP-1

(d) C_m at DP-2

(e) C_p distribution at DP-1

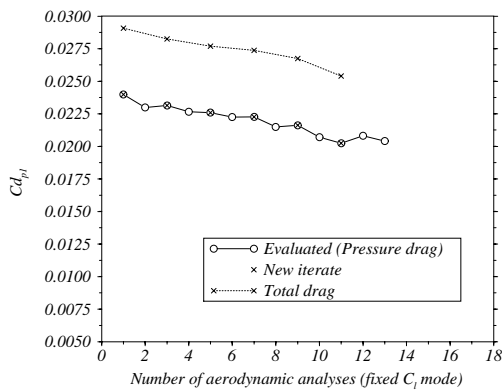(f) C_p distribution at DP-2

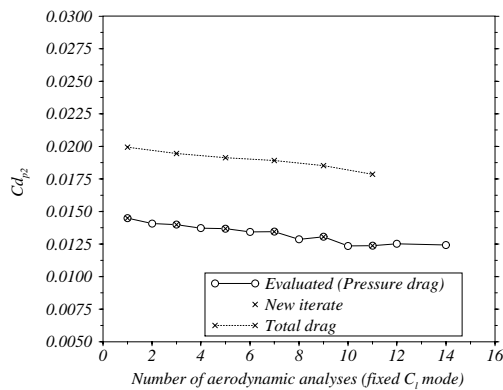Fig. 3   Computational result for Case ME
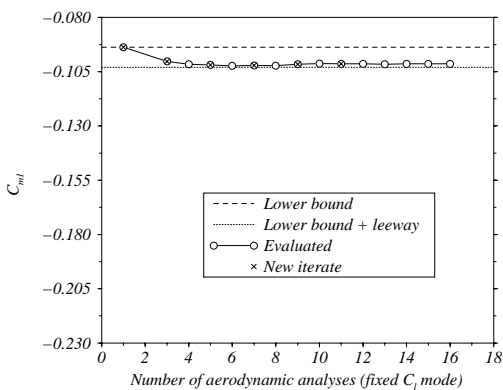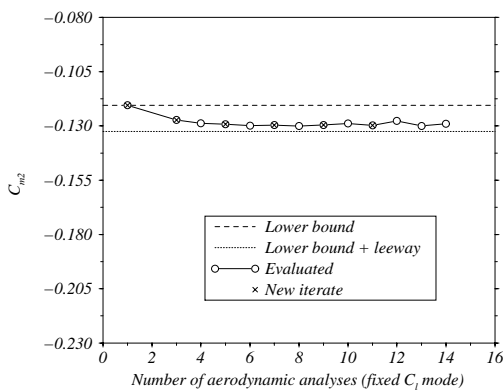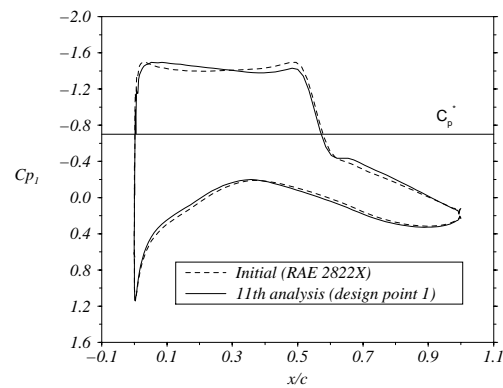
(a) Airfoil geometry

(b) Membership function history

Fig. 4   Computational result for Case ME

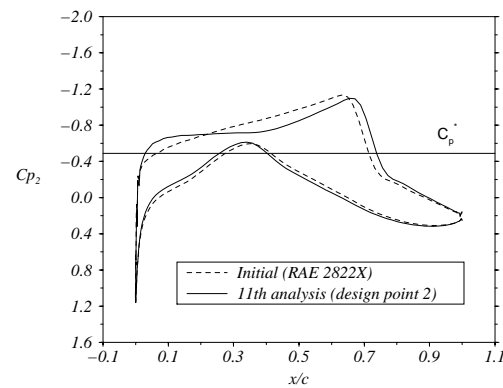(a) C_d at DP-1

(b) C_d at DP-2

(c) C_m at DP-1

(d) C_m at DP-2

(e) C_p distribution at DP-1

(f) C_p distribution at DP-2

Fig. 5   Computational result for Case MN